
Estimation of regional-scale groundwater flow properties in the Bengal Basin of India and Bangladesh

Holly A. Michael · Clifford I. Voss

Abstract Quantitative evaluation of management strategies for long-term supply of safe groundwater for drinking from the Bengal Basin aquifer (India and Bangladesh) requires estimation of the large-scale hydrogeologic properties that control flow. The Basin consists of a stratified, heterogeneous sequence of sediments with aquitards that may separate aquifers locally, but evidence does not support existence of regional confining units. Considered at a large scale, the Basin may be aptly described as a single aquifer with higher horizontal than vertical hydraulic conductivity. Though data are sparse, estimation of regional-scale aquifer properties is possible from three existing data types: hydraulic heads, ^{14}C concentrations, and driller logs. Estimation is carried out with inverse groundwater modeling using measured heads, by model calibration using estimated water ages based on ^{14}C , and by statistical analysis of driller logs. Similar estimates of hydraulic conductivities result from all three data types; a resulting typical value of vertical anisotropy (ratio of horizontal to vertical conductivity) is 10^4 . The vertical anisotropy estimate is supported by simulation of flow through geostatistical fields consistent with driller log data. The high estimated value of vertical anisotropy in hydraulic conductivity indicates that even disconnected aquitards, if numerous, can strongly control the equivalent hydraulic parameters of an aquifer system.

Keywords Bangladesh · India · Inverse modeling · Parameter estimation · Geostatistics

Introduction

Elevated levels of dissolved arsenic in groundwater of the Bengal Basin are causing widespread poisoning of millions of people in India and Bangladesh who rely on wells for drinking water supply. This crisis has prompted numerous studies of the hydrogeochemical processes that lead to arsenic release from sediments as well as development of mitigation technologies such as filters, which, though effective, are not widely used. The distribution of dissolved arsenic in aquifer sediments is not uniform; however, deep groundwater (greater than ~150 m depth) is consistently low in arsenic (BGS and DPHE 2001; Van Geen et al. 2003; Ravenscroft et al. 2005). The deep low-arsenic groundwater may be a viable source of safe drinking water, but evaluation of sustainability requires analysis of the entire Bengal Basin aquifer system and large-scale groundwater flow patterns.

Numerical modeling of groundwater flow can provide quantitative insight into sustainability (e.g., Michael and Voss 2008), but requires input of hydrogeologic properties and aquifer structure that are not fully known throughout the Basin. Moreover, the very large scale of the system, which spans hundreds of kilometers, requires simplification and estimation of equivalent (in the sense of Sanchez-Vila et al. 2006) hydrogeologic properties that, when used in a groundwater flow model, would produce flow patterns that closely approximate the true flow patterns on the temporal and spatial scale of interest.

Accurate estimation of groundwater model parameters can be difficult, particularly for very large aquifer systems with limited data. Because of this, parameters are best estimated using all available data, including geologic knowledge and hydraulic, geochemical, and lithologic measurements. Each type of data provides information on different parts of the aquifer system and over different support volumes. Hydraulic heads reflect diffuse properties over a volume of influence, groundwater age is influenced by flowpaths to measurement locations, lithologic observations are point information in space, and geologic knowledge informs understanding of trends, zones, and aquifer architecture. Different types of data are used to estimate parameters in different ways. Inverse modeling incorporates hydraulic

Received: 20 May 2008 / Accepted: 2 February 2009
Published online: 10 March 2009

© Springer-Verlag 2009

H. A. Michael (✉)
Department of Geological Sciences,
College of Marine and Earth Studies,
University of Delaware, Newark, DE 19716, USA
e-mail: hmichael@udel.edu

H. A. Michael · C. I. Voss
US Geological Survey,
431 National Center, Reston, VA 20192, USA

and geochemical data into a groundwater modeling framework to infer parameters that result in the best match between model results and data; such methods have been widely used in groundwater modeling applications (see e.g., Poeter and Hill 1997; Carrera et al. 2005; Sanz and Voss 2006). Properties can also be inferred based on knowledge of geology and lithology, the small-scale heterogeneity of which defines the aquifer fabric, which controls fluid flow on a larger scale. Upscaling literature has addressed many methods to infer equivalent or effective properties from geologic data or knowledge of spatial correlation structures (see e.g., Wen and Gomez-Hernandez 1996; Renard and de Marsily 1997; de Marsily et al. 2005; Sanchez-Vila et al. 2006).

The goals of this paper are: (1) to synthesize geologic knowledge of the Bengal Basin in order to create a simplified conceptual model of the aquifer system architecture, (2) to estimate equivalent hydraulic parameters for this model using all hydrogeologic and sedimentologic data available when this study was being conducted, and (3) to identify particular needs for future data collection that would improve parameter estimates and reduce uncertainty. The paper begins with a discussion of Bengal Basin physiography, sedimentation, and hydrogeology that forms the basis of a conceptual model of homogeneous anisotropy that may vary among regions of the Basin. Three methods for parameter estimation are used, with varying degrees of success, illustrating the effectiveness of each method under data constraints and the utility of types of hydrogeologic data. Lastly, spatial distributions of hydraulic conductivity (K -fields), having the same equivalent regional horizontal and vertical hydraulic conductivity values as estimated from data, are presented in order to corroborate the conceptual model and to better understand the functioning of highly heterogeneous, anisotropic aquifer systems.

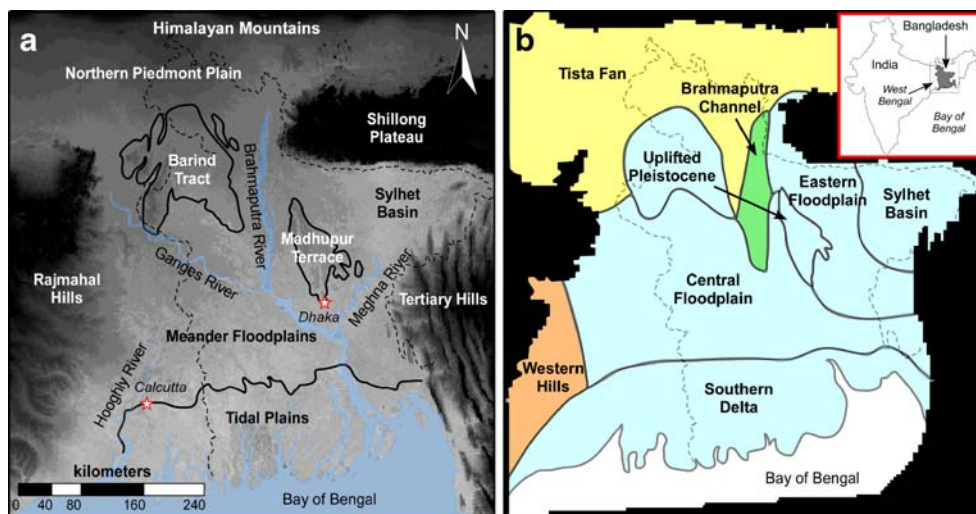
Regional hydrogeology

Physiography

The Bengal Basin lies primarily in Bangladesh and the western portion in West Bengal, India (inset, Fig. 1); the major physiographic and geographic features of the Basin are shown in Fig. 1a. The northern boundary of the Basin is formed by the Himalayan Mountains, the source area for the Ganges and Brahmaputra rivers. On the west, the Basin is bounded by the hard rock Rajmahal Hills, which rise out of the floodplains west of the Hooghly River. In the northeast, the Precambrian Shillong Plateau controls the eastern migration of the Brahmaputra River and supplies sediment to the surrounding floodplains, including the subsiding Sylhet Basin to the south. The major sedimentary geomorphological units of the Basin are Tertiary Hills, Pleistocene Uplands (Barind Tract and Madhupur Terrace), and Holocene Plains, which include the northern piedmont plains, meander floodplains, and the tidal plains of the Southern Delta (MPO 1987, Ahmed et al. 2004).

The Tertiary Hills, a fold belt consisting of a series of N–S trending anticlines and synclines, form the eastern boundary of the Bengal Basin. The sedimentary succession, composed of Quaternary sediments underlain by sequences of shale and sandstone, can be more than 6 km thick and sedimentary units as old as Miocene age have been identified in outcrops (Sikder and Alam 2003). The two major areas of Pleistocene uplands are the Barind Tract in the northwest part of the Basin and the Madhupur Terrace in the central region (Fig. 1). These older alluvial deposits are similar in grain size to recent Basin sediment (Morgan and McIntire 1959) and a thick clay layer covers the surface of both blocks (Ahmed et al. 2004). There are many distinct Holocene plain areas within the Bengal Basin (Ahmed et al. 2004); in general these fluvio-deltaic deposits are characterized by complex patterns of

Fig. 1 Major physiographic regions and geographical features of the Bengal Basin (adapted from Goodbred et al. 2003, EROS 2002; and Persitz et al. 2001). *Dashed line* is the border between India and Bangladesh. **a** *Grayscale* represents elevation of land surface (EROS 2002) and *blue* represents major surface-water bodies. **b** Physiographic regions used in spatial statistical analysis. *Colors* differentiate four regions found to have hydraulic parameter values that are significantly different from the other regions. Inset gives geographic location



unconnected layers of clay, silt, sand, and gravel, creating a highly heterogeneous aquifer architecture.

Geology

The Bengal Basin is one of the largest fluvio-deltaic systems in the world; its sediments extend over an area of 200,000 km² (Uddin and Lundberg 1999) and to depths of more than 20 km (Shamsuddin et al. 2002). The Basin is filled with orogenic sediments deposited by the Ganges-Brahmaputra-Meghna River system that drains an area of more than 1.7 million km² (Allison 1998) and carries an estimated 1×10^9 tons of suspended sediment per year (Coleman 1969). Consideration of stratigraphy and sedimentation give insight into the likely structure of both the small-scale aquifer fabric and the large-scale geometry of layers.

Sediment deposition into the Bengal Basin has occurred since the Late Cretaceous (Johnson and Alam 1990), and sedimentary successions since the Permian have been identified in the western part (Khan 1991; Alam et al. 2003). However, the bulk of sedimentation with relevance to present-day hydrogeology began in the middle Miocene (Uddin and Lundberg 1999; Allison 1998). A generalized description of the vertical stratigraphic sequence in Bangladesh is given in Ravenscroft et al. (2005). Though the general vertical sequence has been described, actual correlation of units is difficult and incompletely known due to similarity of sediment within different strata and a lack of fossil and age data (Sikder and Alam 2003; Uddin and Lundberg 2004). This, in turn, makes it difficult to define, on the basis of geology, sequences of sediments that may be expected to behave as individual confined aquifers within the Basin, should distinct aquifers exist.

Sedimentation processes

Sedimentation of the Bengal Basin has been influenced nearly equally by tectonics, fluvio-deltaic processes, and eustasy, particularly during the Quaternary (Goodbred and Kuehl 2000). The uplift of mountain ranges and large-scale subsidence control Basin geometry, sediment supply and characteristics, and accommodation space for sediment deposition. Compressional deformation and faulting have led to local uplift and subsidence (Morgan and McIntire 1959), influencing river migration and avulsion (Alam et al. 1990; Goodbred et al. 2003).

Tectonic effects are most apparent in the northeastern part of the Basin, though these influences extend to lower delta regions (Goodbred et al. 2003). In the western and central parts of the Basin, fluvial processes control the depositional environment. The Ganges and Brahmaputra rivers are the primary sediment sources, resulting in a high sediment deposition rate, which reached 20 mm per year during the early Holocene (Goodbred et al. 2003). Though both rivers contribute relatively coarse-grained sediment, the steeper gradient of the Brahmaputra distributes sediment with a coarser median grain size than the Ganges

(Kuehl et al. 2005), with expected impact on aquifer properties.

The courses of both the Ganges and Brahmaputra have changed significantly throughout Basin development. The Ganges has tended to migrate slowly eastward, while the braided Brahmaputra channel has experienced more dramatic westward migration and avulsion on a 100-year timescale (Coleman 1969; Allison et al. 2003). Many smaller rivers and streams also flow throughout the Bengal Basin and participate in sediment deposition and erosion while migrating laterally to new channels. River movement has resulted in both formation and erosion of floodplains over time consisting of horizontally oriented layers of sediments with a variety of grain sizes. Maximal layer width is likely restricted to the width of river flood plains in the fluvial-dominated region of the Basin. Subsequent episodes of erosion segmented initially continuous layers into smaller irregular patches.

Development of the lower delta plain is influenced primarily by changes in sea level (Goodbred et al. 2003; Allison et al. 2003). The lower delta plain is characterized by low-lying ephemeral islands and peninsulas separated by tidal channels. The modern lower delta plain developed during the Holocene, likely after the last maximum sea-level transgression at 6,500 BP, when the shoreline was angled from southwest to northeast (Allison 1998).

The controls on development of different parts of the Basin have resulted in variation in Quaternary stratigraphy among the different regions. Overall, the size of grains deposited by rivers decreases downstream, with very coarse sediment deposited in the northernmost Tista Fan (Fig. 1b). In the northeastern region, sequences are dominated by mud, particularly in the quickly subsiding Sylhet Basin (Fig. 1). However, in the fluvially dominated west-central region, sequences are much sandier, with a cap of finer-grained recent sediments near the surface (Goodbred et al. 2003). The lower delta displays alternating fine- and coarse-grained sequences, with muds dominant in the top several meters (Goodbred and Kuehl 2000; Allison et al. 2003).

To summarize, the lateral extent of particular coarse and fine layers is likely quite limited due to the dynamic sedimentation and erosion that formed the Basin, making correlation of stratigraphic units within regions difficult (Umitsu 1993). Despite this, some lateral and vertical trends in aquifer fabrics are likely; these are distinguished in this analysis by physiographic region and vertical variations. An understanding of the processes of Basin formation provides insight into the vertical and lateral structure of the aquifer fabric.

Hydrogeology

Single aquifer or multiple aquifers?

The existence of low-permeability units and the extent to which distinct aquifers are vertically separated are very important to the functioning of the groundwater-flow system. Much of the Bengal Basin hydrogeology literature

refers to a 'shallow' and a 'deep' aquifer, though the location of the contact between these and the effectiveness of a natural hydrologic separation have not been well-defined.

A database of 1950 driller log logs has recently been compiled in a study aimed at mapping the deep aquifers of Bangladesh on a national scale (DPHE 2006). Despite the large amount of data, the heterogeneous nature of the subsurface made it necessary to consider smaller regions individually. Except for a persistent fine-grained surface unit, data demonstrate considerable heterogeneity on the scale on which correlation was attempted.

Thus, descriptions of stratigraphy in the Bengal Basin may be accurate in the local areas where they were developed, but the lateral extent over which these apply is unknown. Stratigraphic differences between study areas and even within particular field sites (e.g., van Geen et al. 2003; BGS and DPHE 2001; JICA 2002) indicate that a single geometric description of confining units cannot be applied regionally. Furthermore, the vast majority of fine-grained units, with the exception, perhaps, of surficial clay and silt layers, appear to be correlated only over short distances throughout most of the Basin. Despite their impact on the groundwater-flow system in reducing the ease of vertical groundwater flow, there is no evidence to suggest that fine-grained units separate sediments into regionally distinct aquifers. This is supported by pumping tests throughout Bangladesh that indicate that at least the top 200 m of sediment behaves as a single, hydraulically connected, and layered aquifer system (MPO 1987).

Previous estimates of hydrogeologic properties

Aquifer tests conducted by the Bangladesh Water Development Board (BWDB) give hydraulic conductivity (K) values that range from 3×10^{-5} to 1×10^{-3} m/s (Hussain and Abdullah 2001), though vertical K values can be orders of magnitude lower (Ravenscroft et al. 2005). Responses to aquifer tests have been leaky-confined in the short term, and unconfined in the long term (Ravenscroft et al. 2005; A. Zahid, BWDB, personal communication, 2007), in agreement with the conceptual model, presented in the preceding, of regionally disconnected confining units. Specific yield values range from 0.02 to 0.19 on average in Bangladesh (BWDB 2002), though much of the Basin has a specific yield in the range of 0.02–0.05 (MPO 1985). Values of specific storage generally range from approximately 10^{-5} m⁻¹ (dense sandy gravel) to 10^{-2} m⁻¹ (plastic clay) for materials in the Bengal Basin aquifer system (Domenico and Schwartz 1998).

Spatial zonation of hydrogeologic properties

Hydrogeologic properties may vary by location because Basin development differed by region as described previously. For example, sediments in the north tend to be coarser, on average, than sediments in the southern delta. The Sylhet Basin, in addition to having a higher proportion of fines than more fluvially dominated areas,

are thought to be highly stratified (Goodbred and Kuehl 2000). Sediment near current or past river locations may have a higher vertical hydraulic conductivity than areas that have been floodplains throughout the formation of the Basin because the low- K fine sediment has been eroded. The marine-dominated deposition in the Southern Delta may have produced more well-preserved fine-grained layers than those in the fluvially dominated regions; one might therefore expect to find more extensive confining units. Each of the broad physiographic regions, described in the preceding, can be divided into multiple sub-regions. Eight regions were chosen for separate parameter estimation based on differences in sedimentation processes that would be expected to lead to differences in hydrogeologic properties. These are illustrated in Fig. 1b: the Southern Delta, Central (Ganges-Brahmaputra River) Floodplain, Eastern (old Brahmaputra and Meghna River) Floodplain, Uplifted Pleistocene (Barind Tract and Madhupur Terrace), Tista Fan, Sylhet Basin, Western Hills of West Bengal, and current Brahmaputra River Channel.

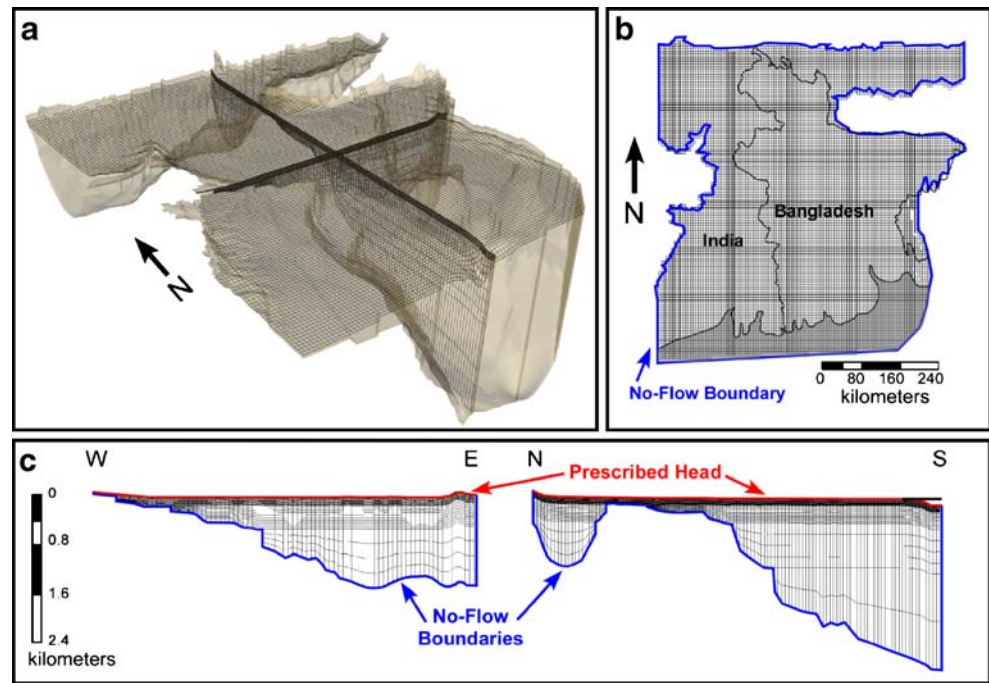
Estimation of regional hydrogeologic parameters

The highly complex and poorly characterized nature of the Bengal Basin aquifer system makes direct representation of subsurface structures in numerical models impossible. However, because each geologic region has a unique mode of development, the system may be approximated as zonally homogeneous, with equivalent hydrogeologic properties that represent the heterogeneity of each region. Three independent methods to estimate the equivalent hydraulic conductivity values of Basin sediments, one of which includes estimation of storage parameters, were used to determine the parameter values that best represent the overall system. Each treats the entire Basin or large regions within it as homogeneous and anisotropic. Use of equivalent parameters in basin-scale groundwater flow models has been shown to be appropriate provided the volume over which parameters are equivalent is statistically homogeneous (Zhang et al. 2006), and this is assumed to be true over wide regions of the Bengal Basin.

Model description

A three-dimensional groundwater flow model of the Bengal Basin aquifer system was used in this analysis for the first two parameter-estimation approaches employing inverse numerical modeling based on hydraulic head data and groundwater-age data. A detailed description of the MODFLOW (Harbaugh et al. 2000) model development, based on the hydrogeology of the region, is given in Michael and Voss (2009) and is only briefly summarized here. The model, shown in Fig. 2, encompasses all of the permeable sediments of the Basin, down to a consistent shale layer where it could be identified, or the Precambrian basement; the maximum depth is approximately 3,000 m and the minimum 100 m below ground surface. The sides and bottom of the model are assumed

Fig. 2 Illustration of model geometry, grid, and boundary conditions. **a** Three-dimensional view of model domain. Vertical exaggeration is 100×. **b** Top view of model grid. Boundary between India and Bangladesh is shown for reference. Sea floor cells are shaded *gray*. **c** Vertical cross-sections and boundary conditions, locations shown in **a**



impermeable to flow, thus boundary conditions of zero flux are assigned to them. The top of the model is the elevation of the land surface, determined from the Shuttle RADAR Topography Mission (SRTM) data (EROS 2002). For steady-state simulations (used for parameter estimation with groundwater ages), the top boundary condition is taken as a prescribed hydraulic head at the land surface elevation, which approximates the water-table elevation throughout the year (Michael and Voss 2009). For transient simulations (used for inverse modeling with hydraulic heads), only major rivers and water bodies are assigned prescribed hydraulic head at the elevation of the land surface. Offshore, the hydraulic head is prescribed as the freshwater equivalent head, equal to the density of seawater (1.025 kg/L) multiplied by the depth of the sea floor. A very low value of hydraulic conductivity (1×10^{-12} m/s) was assigned to the sea floor boundary at water depths greater than ~10 m to represent deposition of very fine sediment; this reduces the impact of the offshore boundary condition on the aquifer system. A detailed discussion of Bengal Basin hydrology and model sensitivity that supports the boundary condition assumptions is given in Michael and Voss (2009).

Automatic inverse modeling using hydraulic head measurements

The first approach to parameter estimation is traditional inverse modeling using time-varying hydraulic head data. BWDB measured the level of the water table weekly in hundreds of shallow wells across Bangladesh. This data set is potentially useful for inverse modeling, in which parameter values are varied to optimize the fit between modeled and measured hydraulic heads. The *Observation*,

Sensitivity, and Parameter-Estimation Processes (Hill et al. 2000) were used with MODFLOW for this analysis.

Approach

The four parameters to be estimated are K_h and K_v , specific yield (Sy), and specific storage (Ss) of the aquifer. These may vary with location, and can be estimated by creating regions within the model and separately evaluating the parameters. If these parameters change among the eight physiographic regions depicted in Fig. 1b, then there are four parameters for each region, for a total of 32 parameters that might be estimated.

Ideally, the entire period of measurement would be simulated, with seasonal recharge and current pumping rates contributing to a seasonal fluctuation of the water table that could be matched to observations. However, the magnitude of and temporal variation in recharge is difficult to quantify, yet the effect on measured heads is potentially greater than the effect of the estimated parameters. Rather than dealing with the uncertainty of recharge during the monsoon season, only the observed head drop during the dry season of 2002–2003 was used for comparison to the modeled dry season.

For inverse modeling, the initial hydraulic head condition was set to the model topography, assumed to represent the level of the water table after the monsoon season because monsoonal recharge fills the aquifer each year nearly everywhere in the Basin (see discussion in Michael and Voss 2009). Observations to be matched during inverse modeling were the measured drop in the water table at each of 141 data points (Fig. 3) located 0.5–10 m below land surface and the time between each maximum and minimum water level. Spatially distributed domestic and irrigation pumping rates were estimated

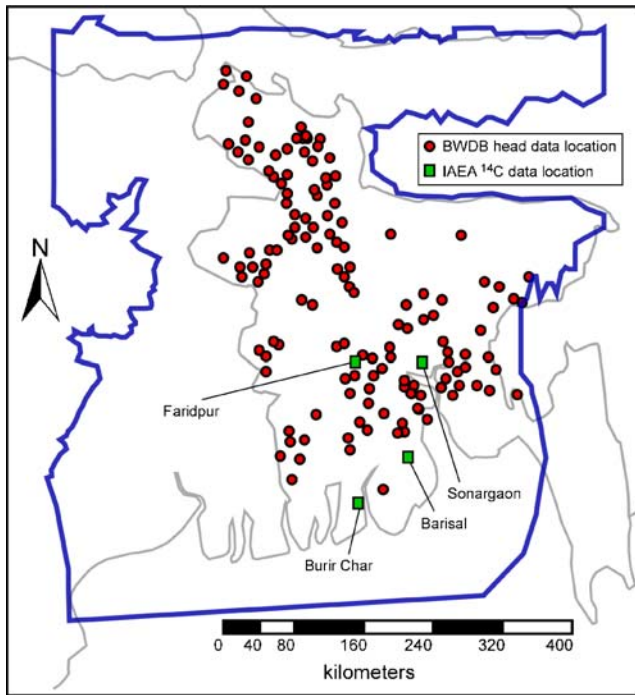


Fig. 3 Hydraulic head data (BWDB 2002) and ^{14}C age data (Aggarwal et al. 2000) locations used for model calibration. Blue line is model boundary

from population data and assumed per capita water use, irrigated area in Bangladesh with an assumed yearly irrigation depth, and irrigation pumping rates in West Bengal, India (Michael and Voss 2009). Pumped water was extracted and zero distributed recharge was assumed throughout the simulated dry season. Recharge occurred only as inflow from prescribed heads at locations of major rivers and large bodies of water, set at the level of the topography on the top surface of the model.

Sensitivity

The success of inverse modeling for parameter estimation depends strongly on the sensitivity of the simulated values of the shallow hydraulic heads at the observation points to parameters being estimated. Absolute values of sensitivity (to 1% changes in values of the four target parameters, beginning from the final estimated value) of simulated hydraulic heads at a shallow (8 m depth) and deep (92 m depth) horizon are mapped in Fig. 4. Blue color indicates regions of zero sensitivity, in which measurements of head would give no information on the parameter. In the Bengal Basin, heads deeper in the aquifer are more sensitive to S_s , K_v , and K_h (Fig. 4a, b, and c) than shallow heads, which are more sensitive to values of specific yield.

Results

The simultaneous estimation of more than three parameters for the entire aquifer was not possible because available hydraulic head measurements are all at or near

the surface, where sensitivities to S_s , K_v , and K_h are lowest. Only 3 parameters could be confidently estimated, rather than the 32 parameters necessary for complete zonation. Estimates of values of the four main parameters were obtained by fixing a value of one parameter and automatically estimating the values of the other three. Several iterations of this process produced a good fit when S_s was fixed at $9.4 \times 10^{-5} \text{ m}^{-1}$ and values of S_y , K_h , and K_v were automatically estimated to be 0.11, $5.2 \times 10^{-4} \text{ m/s}$, and $1.4 \times 10^{-8} \text{ m/s}$, respectively.

The correlation between pairs of parameters is low (maximum value 0.35, for K_h and K_v), which is desirable for independent parameter estimation. The distribution of residuals (difference between simulated and observed values at corresponding times after the peak hydraulic

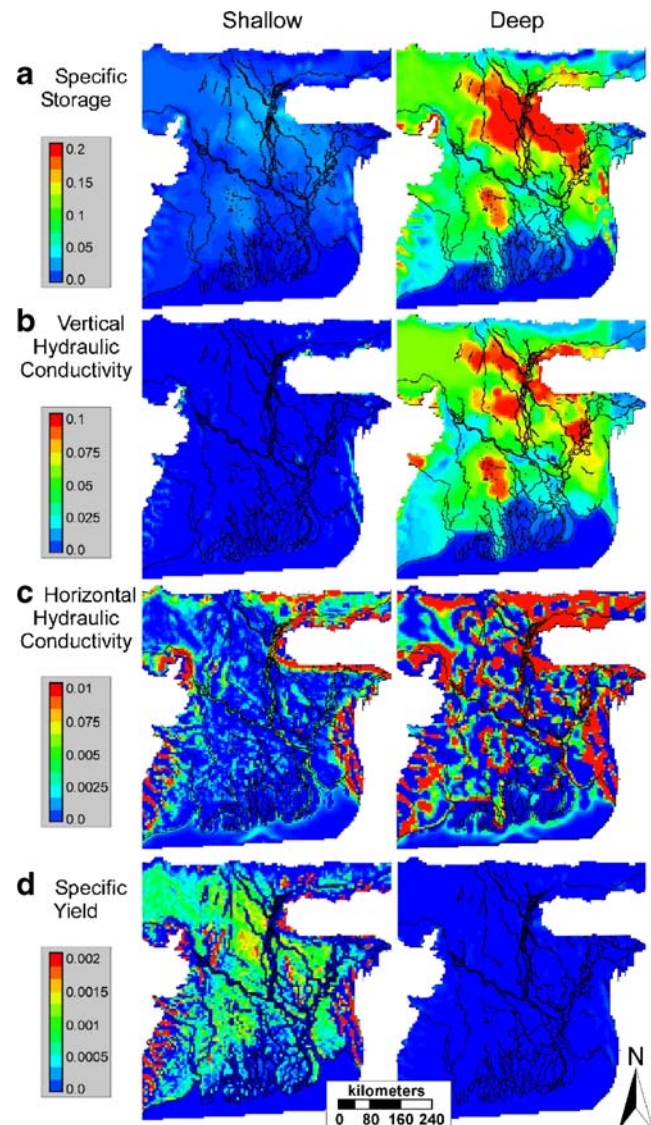


Fig. 4 Sensitivity maps. Colors indicate absolute values of sensitivity of hydraulic head (m) to 1% changes in parameter values. Black lines indicate constant head boundaries along the land surface. Left panels display sensitivities 8 m below the topographic surface and right panels display sensitivities 92 m below the surface. Note difference in scales between parameters, which are shown in order of highest to lowest sensitivity

head or aquifer-full condition) exhibits a spatial trend with location, indicating that zonation of parameters might result in a better fit. Results are insensitive to the coastal boundary condition, as parameter estimates differed in, at most, the fourth decimal place between alternative models with either freshwater equivalent head or a prescribed head of zero at the seafloor.

Limitations

The simplifications involved in this estimation may limit its applicability. Error is introduced by use of estimated values in the model such as pumping rate, and also by incomplete spatial data coverage and a sensitivity too low to allow parameter estimation by region. The model scale may prevent accurate simulation of the seasonal water-table drop in particular places. Each model grid cell is 5 km × 5 km, but the water table may respond to local forcing on a much smaller scale. For example, the proximity of particular pumping wells (there may be several thousand per grid cell area) or the rise and fall of nearby streams are likely to have considerable impacts on the shallow flow system. While a large-scale model is most appropriate for simulating the deep system, it cannot capture the small-scale flows that may be most important to water-table dynamics on a short timescale. Thus, inverse modeling based on heads is best done in large-scale models using deep measurements that are affected by forcing on the scale of the model representation. The analysis would certainly be improved by additional measurements, particularly in deeper parts of the aquifer, in areas with high sensitivity, and also in areas outside of Bangladesh, where such data were not available.

Manual parameter estimation from groundwater-age interpretations

Groundwater age estimates may provide a strong basis for estimating equivalent regional parameters. In particular, the sensitivity of modeled groundwater age to anisotropy in conductivity (defined as Kh/Kv) is found to be very high. In this study, when using ages as data, only Kh and Kv are estimated, as these are the only parameters that control flow over long time periods. For this analysis, MODPATH (Pollock 1994) was used with MODFLOW to predict paths and travel times of groundwater flow. Other studies have used groundwater ages for model calibration, often incorporated with other types of data in an automated (e.g., Hunt et al. 2006) or semi-automated (e.g., Sanford et al. 2004) procedure that varies parameters to minimize an objective function, which quantifies the difference between measured data and modeled results. In the Bengal Basin simulations, changes in parameter values resulted in very different flowpath lengths and recharge locations, making automation difficult using MODPATH. Instead, parameter values were varied manually, and the objective function defined as a discrete quantification of model fit to the data, as explained in the following.

An isotopic and geochemical analysis by the International Atomic Energy Agency (IAEA) includes carbon-14 (^{14}C) and helium-tritium measurements in approximately 30 locations in Bangladesh (Aggarwal et al. 2000). These measurements can be interpreted as groundwater ages by several methods. Many of the groundwater samples taken from depths of less than 100 m contained tritium and were estimated to be less than 100 years old. There were five deep (100–335 m below ground surface) groundwater samples at four sites with ^{14}C measurements from which ages could be interpreted. The uncorrected ^{14}C ages for the five samples range from 5,550 to 21,000 years, and the ages, corrected for geochemical reactions using the Fontes and Garnier (FG) model (Fontes and Garnier 1979), range from 1,620 to 14,500 years (L.N. Plummer, US Geological Survey, personal communication, 2005).

Only deep age interpretations were used in calibration in order to focus analysis on the deep groundwater system containing older waters that have not been greatly affected by the shallow pumping of the last 30 years. Older waters were recharged and aged primarily during predevelopment times and the recent onset of shallow pumping has little disturbed the distribution of deeper water. The deeper pumping that currently takes place affects flowpaths in the vicinity of the deeper wells, possibly reducing the age over that of predevelopment conditions. However, deeper pumping is uncommon and its impacts are considered negligible for the current analysis. Travel times were studied in a steady-state simulation without pumping, and with a prescribed head condition at the elevation of the topography everywhere on the top surface. Kh and Kv values, uniform for the entire aquifer, were varied to find the best match of simulated travel times and groundwater age interpretations. K values were adjusted within reasonable ranges for the aquifer system, and trends in simulated age with changes in Kh and Kv guided the selection of values. Porosity was assumed constant and equal to 0.2, a value higher than the specific yield calibrated from head measurements (described in the previous section) because the water is primarily flowing through sandy main aquifer sediments, while specific yield applies only to the zone of water-table fluctuation at the surface, which is generally finer-grained.

Results

For each of 75 parameter combinations, model run results were scored based on the goodness of fit between simulated and interpreted groundwater ages. The scoring system, a discrete objective function to be maximized, is one point for an age between the unadjusted and the FG-adjusted age (because of uncertainties in both and effects of current deep pumping), one half point for an age outside of but within 1,000 years of the age range, and negative one point for an age more than 10,000 years outside of the estimated age range. Two parameter combinations (indicated by yellow diamonds in Fig. 5) allowed the model to fit all five interpreted ages, for a maximum score of 5. A region of successful parameter

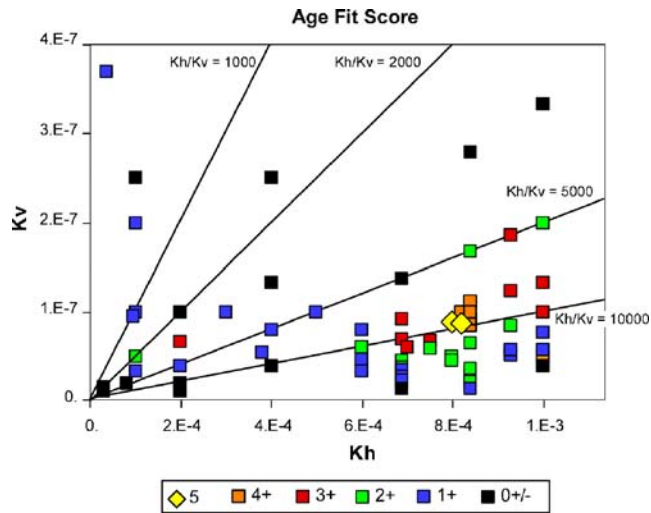


Fig. 5 Model calibration with groundwater-age interpretations from ^{14}C data. Age-fit scores for each simulation are plotted as a function of values of vertical and horizontal hydraulic conductivity. Lines of constant anisotropy values are shown

combinations surrounds this pair, clearly indicating a region of parameter space in which the optimal values occur. The best-fitting pairs are $Kh=8.0 \times 10^{-4}$, $Kv=8.9 \times 10^{-8}$ m/s and $Kh=8.2 \times 10^{-4}$, $Kv=8.7 \times 10^{-8}$ m/s, resulting in values of anisotropy of 8,989 and 9,425, respectively. A change of less than 3% to either parameter results in a fit with a score of less than 5.

The sensitivity of groundwater ages to Kh and Kv is high in the modeled system, as evidenced by the very narrow range of parameters that results in ages near the interpreted values. Increasing both Kh and Kv by an order of magnitude decreases the age at each point by an order of magnitude, but does not change the flow pattern. Increasing or decreasing Kh or Kv individually changes the flow patterns and ages significantly, but in a non-uniform manner, increasing some ages and decreasing others.

Limitations

The simplifications in this set of simulations are significant and assumptions are made regarding the meaning of interpreted groundwater ages. A constant porosity is assumed throughout the Basin and its value may be considered as a scaling factor for modeled water age. Further, age estimates are up to 21,000 years. During this time period, both climate and hydraulic gradients have changed significantly. Moreover, Holocene sediment, more than 100 m deep in many areas, was deposited during this period. Thus, the modeled system, constructed according to present-day predevelopment conditions, may not accurately reflect conditions in the past. Additionally, the age of the flowing groundwater may be different than estimated from ^{14}C measurements and modeling of advective flow only due to the existence of multiple source areas (Pint et al. 2003), diffusive and slow-flow contributions (Sanford 1997; Bethke and Johnson 2002) or to pumping-induced transient leakage from ^{14}C -dead

zones of low hydraulic conductivity (Zinn and Konikow 2007). However, even given these assumptions, the analysis suffices as an initial evaluation of the few data currently available and demonstrates the utility of deep groundwater age data.

Analysis based on driller logs

Theory and approach

The final approach to estimation was analysis of lithology obtained from driller logs to estimate upscaled, or effective values of Kh and Kv . The lithologic units cannot be correlated over the distances between boreholes, so estimates are based on point-wise analysis. In addition to estimation of anisotropy, this method provides a means to assess statistical differences in parameters among various regions of the Basin.

In a layered system with strata of constant thickness and infinite extent, the direction of highest effective hydraulic conductivity will be parallel to layering with an effective K equal to the arithmetic mean, and the direction of lowest conductivity will be perpendicular to layering, with an effective K equal to the harmonic mean. These are known as Wiener bounds, the maximum and minimum possible values of effective hydraulic conductivity (Renard and de Marsily 1997):

$$\mu_h \leq K_{\text{eff}} \leq \mu_a, \quad \mu_a = \frac{\sum K \cdot d}{\sum d}, \quad \text{and} \quad \mu_h = \frac{\sum d}{\sum d/K}, \quad (1)$$

where K_{eff} is the effective hydraulic conductivity in any direction, K is the hydraulic conductivity of a particular lithologic unit, and d is the thickness of that unit.

The layers in the Bengal Basin system are neither infinite in extent nor constant in thickness, so the effective hydraulic conductivity in the horizontal and vertical directions will lie between the Wiener bounds. One method to obtain estimates of K_{eff} that accounts for finite layer extent is use of the empirical expression suggested by Ababou (1996) for an anisotropic and statistically homogeneous medium:

$$K_{\text{eff}} = \mu_a^\alpha \mu_h^{1-\alpha}, \quad \alpha = \frac{D - \ell_h/\ell_i}{D}, \quad (2)$$

where D is the space dimension, ℓ_i is a length scale for K in the relevant direction, and ℓ_h is the harmonic mean of the length scales in the principal directions of anisotropy.

Calculation of K_{eff} using this method in this three-dimensional analysis requires three values of ℓ_i , one for each principal direction. The length scale is a correlation length for statistically homogeneous log-Gaussian-distributed fields (R. Ababou, Institut de Mecanique des Fluides de Toulouse, personal communication, 2008), of which the Bengal Basin aquifer system is likely not an example.

For simplicity, the vertical length scale, l_z was assigned the mean thickness of the lithologic units in each driller log. Based on understanding of sedimentary depositional processes that formed the Basin, the lateral extent of low- K lithologic units might be as small as an individual stream width (order of 10 m) or as large as the distance between major rivers (order of 50 km). Thus, for this analysis, in the horizontal directions the aquifer system is considered isotropic, ($l_x = l_y$) with assumed length scale less than 50 km but greater than 10 m. It was found that the sensitivity of the average effective anisotropy (Kh/Kv) and hydraulic conductivities to the horizontal length scale decreases with increasing length scale over this range, with little sensitivity at scales greater than 1,000 m on a log scale (Fig. 6). An estimate of 500 m was arbitrarily chosen for the length scale in both principal horizontal directions because anisotropy approaches that of the Wiener bounds (μ_{ah}) at greater length scales, on average, though the average anisotropy at a length scale of 500 m (32,000) is still less than one third the average Wiener anisotropy (98,000). The length scale is not expected to reflect the actual extent of layers in this non-log-Gaussian system.

Greater complexity in statistical description of the Bengal Basin aquifer fabric is possible, though it is not considered in this study. For example, river channels tended to flow from the northwest to the southeast during Basin formation, possibly resulting in longer length scales in that direction. It is also likely that the length scale of low- K layers is greater in the southern part of the Basin than in the northern part because of the differences in depositional environments mentioned in the preceding.

Hydraulic conductivity values were assigned to seven categories chosen for lithology, listed in Table 1, with driller log descriptions assigned to one category each. The

Table 1 Lithologic categories and associated hydraulic conductivity values, the length proportion of all data in each category, and weighted log-mean hydraulic conductivity values for similar lithologies

Lithology	Assigned K [m/s]	Length proportion of data	Weighted log-mean K [m/s]
Gravel	6.0×10^{-3}	0.03	5.2×10^{-4}
Coarse sand	1.1×10^{-3}	0.07	5.2×10^{-4}
Medium sand	5.8×10^{-4}	0.23	5.2×10^{-4}
Fine sand	3.0×10^{-4}	0.29	5.2×10^{-4}
Silt	4.6×10^{-6}	0.01	1.1×10^{-6}
Sandy clay	1.0×10^{-6}	0.14	1.1×10^{-6}
Clay	7.0×10^{-10}	0.23	7.0×10^{-10}

values of hydraulic conductivity were chosen based on literature values specific to the Bengal Basin, where available, or more general estimates for specific lithologies. The K of the clay has the greatest control over the Kv values. This was assigned a value of 7.0×10^{-10} m/s based on an estimate for the Madhupur Clay (Rahman and Ravenscroft 2003). The fine, medium, and coarse sands were assigned K values of 3.0×10^{-4} , 5.8×10^{-4} , and 1.1×10^{-3} m/s, respectively, based on values for gray sediments (usually found in the upper, Holocene part of the aquifer), though the values estimated for brown (generally deeper and of Pleistocene age) sediments are half these values (Rahman and Ravenscroft 2003). The values chosen for sand are consistent with estimates of the Report of the Ground Water Task Force (Hussain and Abdullah 2001), and the value of 4.6×10^{-6} m/s given in that report was assigned to silt. Values for sandy clay, 1.0×10^{-6} m/s, and gravel, 6.0×10^{-3} m/s, were estimated from literature (e.g., Domenico and Schwartz 1998). Where a mixture of two categories was logged, the hydraulic conductivity value from the finer category was assigned.

The analysis involved lithologic data from 147 driller logs from four data sets at locations throughout Bangladesh and West Bengal, India (Fig. 7a), ranging in depth from 30 to 665 m, with a mean depth of 202 m. These include 64 from the Eighteen District Towns Project of the Department of Public Health Engineering in Bangladesh (DPHE 1999), 36 from the Bangladesh Master Plan Organisation (MPO 1985), 14 logs from Goodbred and Kuehl (2000) in both Bangladesh and India, and 33 Geological Survey of India (GSI) driller logs in West Bengal (Deshmukh et al. 1973). The data from each driller log were used according to the method previously described and Eq. 2 to calculate vertical and horizontal values of K_{eff} at each driller log location.

Results

The analysis resulted in effective Kh values ranging from 6.2×10^{-6} to 3.3×10^{-3} m/s, with a log-mean (inverse log base 10 of the mean of the log base 10 of the K values) and a median value both equal to 2.4×10^{-4} m/s. The effective Kv values ranged from 1.4×10^{-9} to 6.5×10^{-4} m/s, with a log-mean of 3.0×10^{-8} m/s and a median value of 9.7×10^{-9} m/s. The point-wise anisotropy (Kh/Kv) values

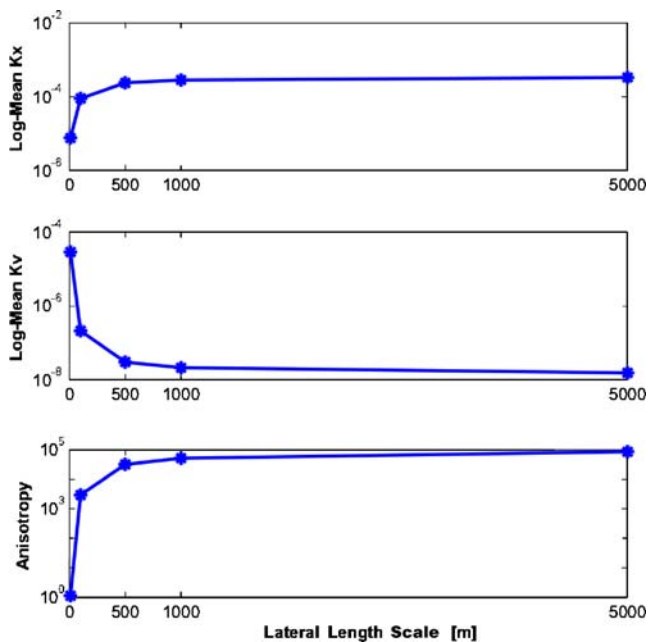


Fig. 6 Mean over all driller logs of calculated log (Kh), log (Kv), and Kh/Kv for five values of lateral length scale

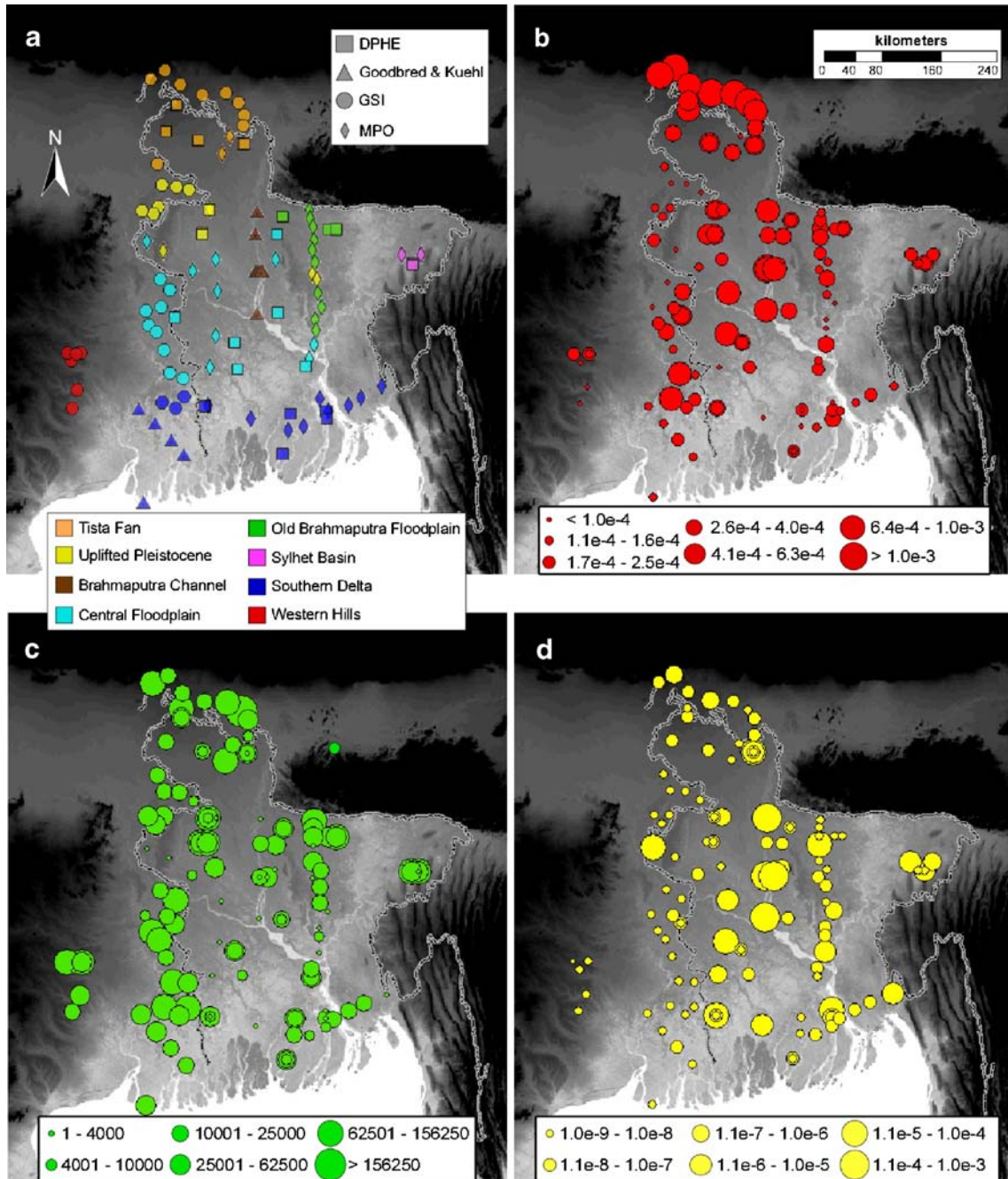


Fig. 7 Driller log parameter analysis data and results. **a** Driller log locations: shapes indicate data set and colors indicate assigned physiographic region, **b** calculated horizontal hydraulic conductivity [m/s], **c** calculated anisotropy, and **d** calculated vertical hydraulic conductivity [m/s]; circle size indicates value range

ranged from 1 to 288,000 with a mean of 32,000 and a median value of 22,000.

Resulting log-mean values of Kh for the four data sets vary by less than a factor of three: DPHE, GSI, MPO, and Goodbred and Kuehl log-mean Kh values are 2.9×10^{-4} , 2.1×10^{-4} , 1.5×10^{-4} , and 4.2×10^{-4} m/s, respectively. The Kv values are more variable, with log-means of 1.7×10^{-8} , 6.6×10^{-9} , 8.7×10^{-8} , and 1.1×10^{-6} m/s, respectively. This disparity could be a result of differences between data sets in the total length or the level of detail of the driller log, as

evidenced by the average thickness of each discrete lithology, or facies thickness. However, there is no clear trend in Kh or Kv with borehole depth or facies thickness in any of the data sets.

It is also possible that the differences between data sets are a reflection of the differences in the locations of the boreholes and true differences in stratigraphy. The calculated horizontal and vertical hydraulic conductivity values and their ratio are mapped in Fig. 7b–d. Though values are highly variable, there appear to be trends with

physiographic region; for example, K_h appears highest in the northern Tista Fan region and along the Brahmaputra River Channel, and lowest in the southern and western parts of the Basin.

The eight physiographic regions of Fig. 1b were selected for statistical comparison of K_v , K_h and anisotropy values. Figure 7a illustrates driller log locations, their data sets, and assigned physiographic region. The results of regional analysis are listed in Table 2.

An analysis of variance (ANOVA) (Devore 2000) for each of the three parameters was done over the eight regions. The F statistic was used for the single-factor ANOVA, which applies for observations from a normal distribution. Because hydraulic conductivity values may fall closer to a log-normal than a normal distribution, log base 10 of the calculated K_h and K_v values were used. Anisotropy was not log-transformed. The data were not perfectly normally distributed, so the application of the ANOVA is only approximate. The null hypothesis that the mean parameter values of all regions are equal is rejected for K_h and K_v at any reasonable level of significance and anisotropy at the 0.05 level of significance.

A Tukey procedure (Devore 2000) was used to identify regions that are significantly different from one another. K_h values were significantly lower in the Western Hills than in all other areas, whereas the Tista Fan and Brahmaputra River Channel have significantly higher K_h values than the other six regions, but not significantly different from each other. The Western Hills region also exhibits the lowest value of vertical hydraulic conductivity, and the Central Floodplain, Tista Fan, and Brahmaputra River Channel have the highest values. K_v values of the Central Floodplain and Tista Fan regions are statistically greater than only the Western Hills, but the Brahmaputra River Channel K_v is significantly greater than all 7 other regions. Anisotropy is lowest in the Brahmaputra River Channel and Southern Delta and highest in the Sylhet Basin and Western Hills. The Sylhet region is statistically different only from the Brahmaputra River Channel, and the Western Hills region has greater anisotropy than both the Southern Delta and Brahmaputra River Channel.

According to the preceding analysis, there is a statistical reason to divide the Basin into only four regions based on K_h and K_v (Fig. 1b). The Western Hills of West

Bengal along the western boundary of the Basin are clearly different from all other regions, with the lowest value of both K_h and K_v , and the highest value of anisotropy. The Uplifted Pleistocene sediments may have been expected to be less permeable than recent Floodplain deposits, but the Floodplain areas, the Southern Delta, and the Uplifted Pleistocene terraces do not have statistically different effective K_h and K_v values. Though lithology is similar in these areas, the K values may be lower in Pleistocene strata because of greater diagenesis (Rahman and Ravenscroft 2003). Given that K values are constant over the regions, such differences are not resolved here. The Tista Fan sediments, as expected due to depositional environment, are coarser than the lower regions of the Basin and are therefore significantly more permeable, yet are highly anisotropic. The Brahmaputra River Channel, however, is highly permeable in both directions, making it less anisotropic than other regions and also statistically different. Though a simplification because the assumed K values were held constant over the Basin, the information regarding spatial differences among regions is perhaps a more valuable result of this analysis than the estimates of parameter values.

Limitations

Differences in the lithologic description between data sets (e.g., differences in the level of detail in recording or the criteria for classification) can create bias in the calculated value of hydraulic conductivity. Though this is likely considering the involvement of a variety of drill-log observers at different places and times in creating these data sets, log-mean values of K_h for the four data sets vary by less than an order of magnitude. A further limitation is that the actual values of K_h and K_v determined from Ababou's relation are dependent on both the assumed values of K for each lithology (particularly the highest and lowest values) and the horizontal length scale, which cannot be estimated from the data.

Regional parameter estimation summary

Each of the three methods used to estimate the hydrogeologic parameters introduces a unique set of assumptions and simplifications that lead to errors in the

Table 2 Mean of point-wise hydraulic conductivity and anisotropy values calculated for physiographic regions of the Bengal Basin by driller log analysis

Physiographic region	Number of driller logs	Log-mean K_h [m/s]	Log-mean K_v [m/s]	Mean K_h/K_v	Statistical region	Log-mean K_h [m/s]	Log-mean K_v [m/s]
Western Hills	6	7.0×10^{-5}	2.1×10^{-9}	60,366	1	7×10^{-5}	2.1×10^{-9}
Uplifted Pleistocene	21	1.9×10^{-4}	8.3×10^{-9}	38,868	2	1.9×10^{-4}	1.8×10^{-8}
Eastern Floodplain	17	1.7×10^{-4}	1.5×10^{-8}	29,593	2	1.9×10^{-4}	1.8×10^{-8}
Sylhet Basin	10	2.3×10^{-4}	2.1×10^{-8}	50,149	2	1.9×10^{-4}	1.8×10^{-8}
Southern Delta	31	1.7×10^{-4}	2.3×10^{-8}	21,252	2	1.9×10^{-4}	1.8×10^{-8}
Central Floodplain	30	2.2×10^{-4}	3.2×10^{-8}	26,278	2	1.9×10^{-4}	1.8×10^{-8}
Tista Fan	23	5.5×10^{-4}	3.8×10^{-8}	40,975	3	5.5×10^{-4}	3.8×10^{-8}
Brahmaputra River Channel	9	7.9×10^{-4}	2.2×10^{-5}	7,419	4	7.9×10^{-4}	2.2×10^{-5}
Log-mean (K_h , K_v); Mean (K_h/K_v)		3.0×10^{-4}	2.7×10^{-6}	34,363	Log-mean	2.3×10^{-4}	3.7×10^{-8}

estimates. Each method also considers a different part of the aquifer system and therefore would be expected to result in different estimates even without errors. The spatial analysis indicates that the structure of the Bengal Basin aquifer system is not statistically homogeneous, calling into question the results of the inverse modeling which produced single values for the entire Basin. Despite this, because hydraulic head and age data used in inverse modeling are primarily located in the central part of the Basin, within the floodplain areas, lower delta, and Pleistocene terraces, which were not shown to be statistically different from each other, the inverse methods provide an estimate of the parameters in the largest part of the Basin. The possible deviations of the other regions from the central Basin parameter estimates can be assessed based on the spatial analysis.

Consideration of the sensitivity of each data type to estimated parameters, the uncertainties associated with using each type of data, and the part of the system for which each gives information allows assessment of the utility of hydraulic head, groundwater age, and driller log data in regional-scale parameter estimation. Inverse modeling based on shallow hydraulic heads informs estimation of shallow parameters. Heads measured at greater depths would provide information about a larger part of the system, potentially increasing the parameter sensitivity, the accuracy of the estimates, and the number of individual parameters that can be distinguished. Groundwater age estimates derived from isotope measurements are subject to uncertainty in interpretation, and inverse modeling to match ages introduces simplifications that may lead to inaccuracy. However, sensitivity of ages to hydraulic conductivity values is very high, and even a few deep age measurements can be used to estimate equivalent parameter values with some degree of confidence. Additional age estimates would further constrain the parameters and potentially allow estimation of more than two Basin-wide values. Driller log analysis incorporates details and physical data not considered in a large-scale model, but important information on the lateral continuity of layers is not available, data coverage is sparse, and the depth range of information is limited. However, information at single locations distributed over the Basin allows comparison of estimated parameters between physiographic regions, which was not possible using inverse modeling methods with the available data.

Despite the potential shortcomings of each method, hydraulic conductivity estimates agree well, differing by less than an order of magnitude (Table 3). K_h values from

inverse modeling are intermediate between values for fine and medium sand (from hydraulic heads) and between medium and coarse sand (from groundwater ages) assumed in the driller log analysis. Point-wise estimates of K_h from the driller log analysis are highly variable and range from between assumed values of sandy clay and silt to values between coarse sand and gravel. K_v values estimated from inverse modeling are intermediate between assumed K values for clay and sandy clay. The driller log analysis estimates of K_v are also highly variable, ranging over more than five orders of magnitude, from values lower than that of sandy clay to higher than that of medium sand.

Intermediate values among K_h and K_v estimates are chosen as most representative for use in forward modeling, and these indicate a relatively high vertical anisotropy for the Basin sediments. The best guess values for the large-scale equivalent properties of the system used for study in Michael and Voss (2008, 2009) are: $K_h=5 \times 10^{-4}$ m/s, $K_v=5 \times 10^{-8}$ m/s, $K_h/K_v=10,000$. Similar values of large-scale vertical anisotropy have been estimated in sedimentary aquifers in the United States, including the Gulf Coast aquifer system, which includes the Mississippi River Valley alluvial aquifer ($K_h/K_v \sim 50,000$, ranging from 530 to 210,000) (Williamson et al. 1990), and the Espanola Basin in New Mexico ($K_h/K_v \sim 100\text{--}20,000$) (Keating et al. 2005). The sensitivity of the flow system to the selected base-case parameter values is considered in the modeling analyses (Michael and Voss 2008, 2009).

Conceptualization of heterogeneity using a geostatistical field

An aquifer system conceptualization in which low- K layers are discontinuous throughout the Basin raises the question of whether these units can actually produce a high vertical anisotropy in regional hydraulic conductivity of 10,000:1. This was tested by generating geostatistical fields that display 10,000:1 anisotropy. Three fields were generated that are conceptually acceptable representations of the aquifer fabric, consistent with available data. Horizontal and vertical flow through them were simulated, in order to estimate equivalent values of K_h and K_v for varying lengths of horizontal spatial continuity. Similar analyses of simulated flow through heterogeneous random fields have been done to develop and test empirical and

Table 3 Hydrogeologic parameter estimates by three methods and selected best estimate values

Method	K_h [m/s]	K_v [m/s]	K_h/K_v
Driller log analysis	6×10^{-6} – 3×10^{-3} Log-mean= 2×10^{-4}	1×10^{-9} – 7×10^{-4} Log-mean= 3×10^{-8}	1.2–288,000 Mean=32,000
Inverse modeling–hydraulic heads	5×10^{-4}	1×10^{-8}	37,000
Inverse modeling–groundwater ages	8×10^{-4}	9×10^{-8}	9,000
Best estimate	5×10^{-4}	5×10^{-8}	10,000

analytical expressions for effective K (e.g., Naff et al. 1998; Sarris and Paleologos 2004).

Geostatistical generation of heterogeneity

The software SGEMS (Remy 2004) was used to generate spatial distributions of heterogeneous lithology (fields) using the geostatistical method, Sequential Indicator Simulation (SISIM; Journel and Alabert 1990). SISIM can be used to generate fields of categorical (indicator) variables based on the relative proportion of each category and their spatial correlation. The driller log data used in the preceding analysis were used to obtain the input information. The seven lithologic categories of the driller log analysis were reduced to three for simplicity in simulation by combining those with similar K values: sand and gravel, silt and sandy clay, and clay.

The spatial correlation of the simulated field is input into SISIM as a (semi-)variogram (γ), a measure of the difference in data values as a function of spatial separation distance. The experimental variogram was obtained from the driller log data, calculated according to the equation:

$$\gamma(u, u + h) = \frac{1}{2n} \sum_{i=1}^n [I(u_i + h) - I(u_i)]^2, \quad (3)$$

where n is the number of data pairs, \mathbf{h} is the separation vector between data locations μ_i and $\mu_i + \mathbf{h}$, and I are indicator values for each lithologic category, k , where:

$$I(u, k) = \begin{cases} 1 & \text{if } Z(u) = k \\ 0 & \text{otherwise} \end{cases}, \quad (4)$$

and Z is the categorical variable.

Only the variogram in the vertical direction could be calculated from the data because the horizontal separation distance between well locations is too great for estimation of the horizontal variogram. The experimental variogram cannot be input directly into the simulation algorithm; rather a variogram model with acceptable mathematical form is fit to the data and used as input. The best fit variogram model incorporates a nugget effect (variability at zero separation distance) and an exponential component, expressed as:

$$\gamma(h) = c_n + c_e \left[1 - \exp\left(\frac{-3h}{a}\right) \right], \quad (5)$$

where \mathbf{h} is the vertical linear separation distance between two points, a is the practical range, the distance at which the variogram is at 95% of the maximum, and c_n and c_e are the variance contributions for the nugget and exponential components, respectively (Goovaerts 1997). The vertical experimental (from driller logs, subsampled at 1-m intervals) and model indicator variograms for each lithologic category are shown in Fig. 8.

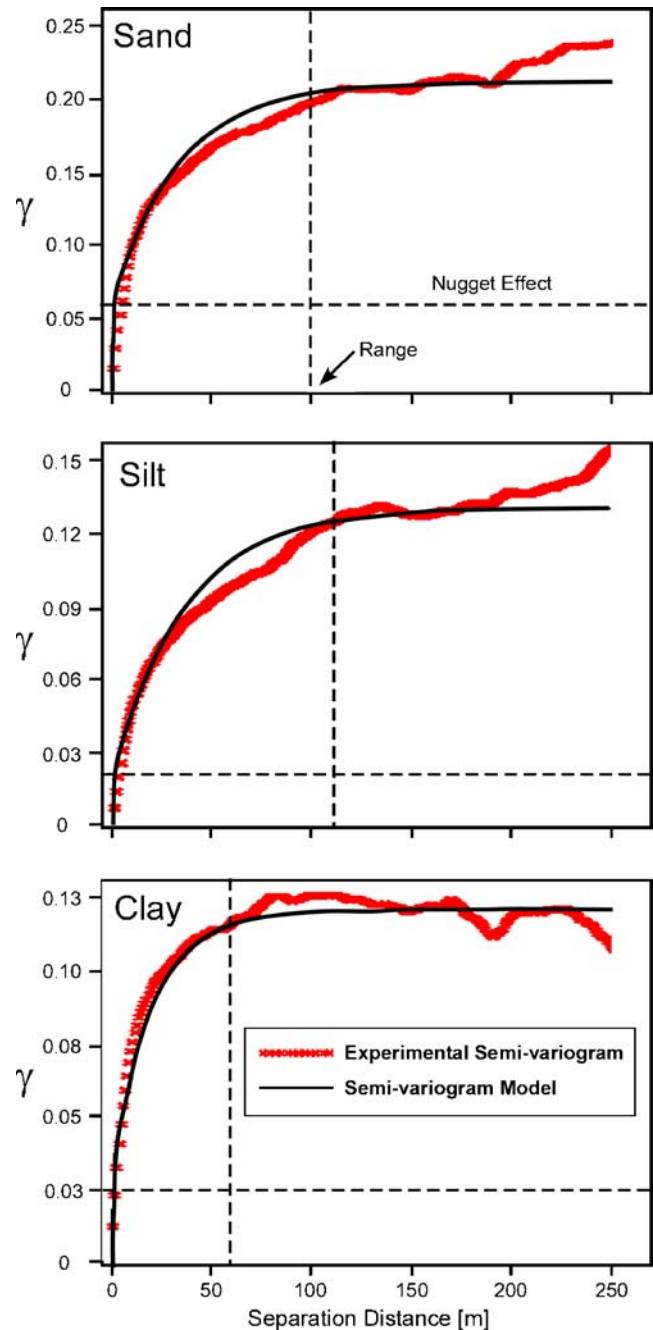


Fig. 8 Experimental and model indicator variograms for three lithologic categories of driller log data

Geostatistical fields were generated with SISIM onto grids with 50×50 cells horizontally and 600 cells vertically. For generation, each cell was $5 \text{ m} \times 5 \text{ m} \times 1 \text{ m}$, but the horizontal dimension was rescaled post-generation, as described in the following. Three fields were generated with identical input statistics, obtained from data (Table 4). Resulting statistics (category proportions and variogram model coefficients) are given in Table 4 and images are shown in Fig. 9. Overall, the statistics of the generated fields are consistent with the data, though the nugget

Table 4 Category proportions and vertical variograms for driller log data and three geostatistical fields generated with sequential indicator simulation

	Lithology	Category proportions	Vertical variogram model		
			Nugget (c_n)	Exponential contribution (c_e)	Range (a) [m]
Data	Sands and gravel	0.62	0.06	0.15	100
	Silt and sandy clay	0.15	0.02	0.11	110
	Clay	0.23	0.03	0.09	60
Field 1	Sands and gravel	0.59	0.10	0.15	100
	Silt and sandy clay	0.14	0.06	0.11	110
	Clay	0.27	0.09	0.09	95
Field 2	Sands and gravel	0.63	0.08	0.17	100
	Silt and sandy clay	0.16	0.05	0.08	110
	Clay	0.21	0.11	0.09	70
Field 3	Sands and gravel	0.58	0.10	0.12	95
	Silt and sandy clay	0.19	0.05	0.09	100
	Clay	0.24	0.08	0.09	60

component of variability in the generated fields is somewhat higher.

Flow simulation and equivalent properties

The lithology fields were converted to hydraulic conductivity fields (K-fields) by assigning to each the mean of the log of the assigned K values weighted by the length along the driller log of each lithology found in the data (Table 1).

MODFLOW was used to simulate groundwater flow horizontally and vertically through the three K-fields. A hydraulic gradient of 0.02 was assigned across two opposite model faces (sides for horizontal, and top and bottom for vertical), with all other faces as no-flow boundaries. The flow through the system induced by the gradient was determined as model output and used to calculate the equivalent Kh and Kv according to Darcy's law. The horizontal extent of each K-field, or flow model,

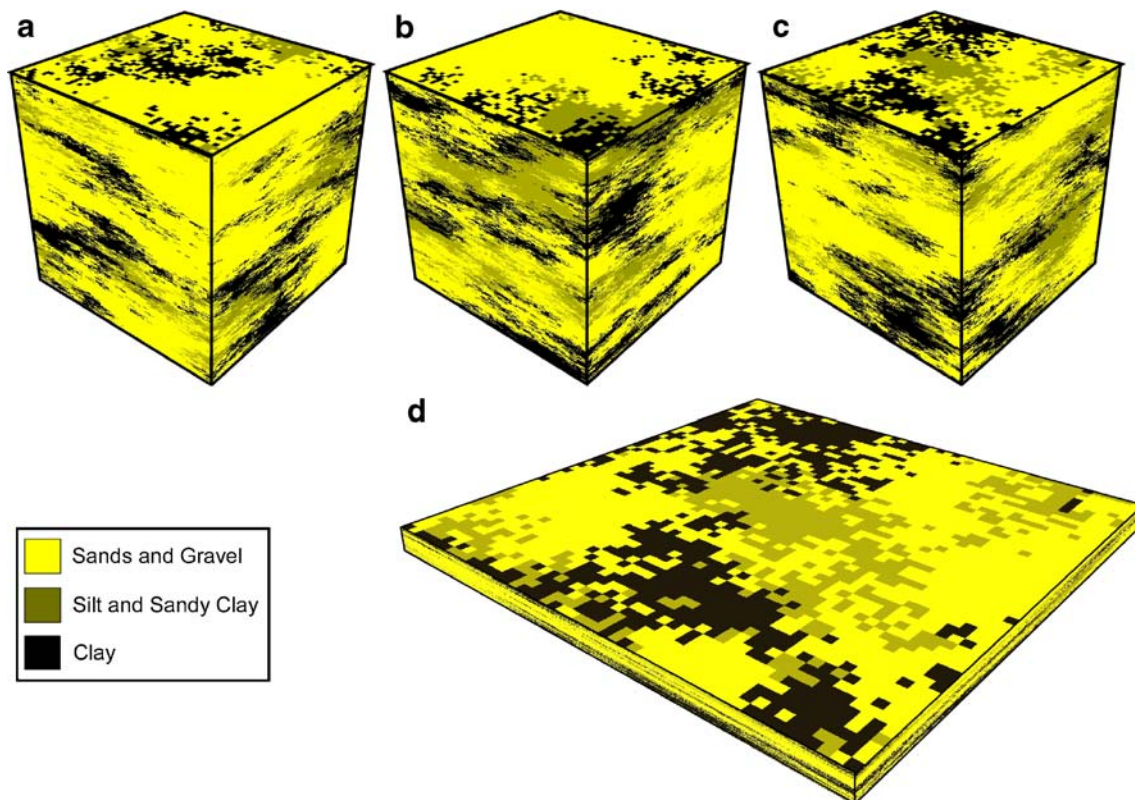


Fig. 9 Geostatistical fields generated with sequential indicator simulation using statistics based on driller log data. Colors represent lithologic category. **a** Field 1, dimensions are 250 m × 250 m × 600 m; **b** Field 2, dimensions as in **a**; **c** Field 3, dimensions as in **a**; **d** Field 3, dimensions are 20 km × 20 km × 600 m

Table 5 Flow simulation results for the three geostatistical fields with varying horizontal extent

	Grid Size	Kh (m/s)	K_v (m/s)	Kh/K_v	Kh/K_v ratio ^a
Field 1	20×20 km	1.8E-04	5.6E-08	3,155	2.9 ^b
	40×40 km	1.8E-04	2.0E-08	9,160	
	60×60 km	1.9E-04	1.2E-08	15,547	2.3 ^c
	80×80 km	2.0E-04	9.2E-09	21,480	
Field 2	20×20 km	2.1E-04	1.3E-07	1,608	2.9 ^b
	40×40 km	2.2E-04	4.7E-08	4,650	
	60×60 km	2.3E-04	2.7E-08	8,426	2.7 ^c
	80×80 km	2.3E-04	1.8E-08	12,468	
Field 3	20×20 km	1.8E-04	1.1E-07	1,668	3.3 ^b
	40×40 km	1.9E-04	3.4E-08	5,457	
	60×60 km	1.9E-04	1.9E-08	10,280	2.8 ^c
	80×80 km	2.0E-04	1.3E-08	15,358	

^a Kh/K_v Ratio is the ratio of anisotropy of fields with double horizontal extent

^b 40 km×40 km divided by 20 km×20 km Kh/K_v

^c 80 km×80 km divided by 40 km×40 km Kh/K_v

was varied from 20 to 80 km along each side (by rescaling the lateral dimensions accordingly), but the number of cells remained constant and the K values in each remained the same (i.e., the K -fields were ‘stretched’ horizontally).

The horizontal and vertical values of equivalent hydraulic conductivity calculated from flow simulations through the three K -fields with different lateral extents are given in Table 5. K_v values consistently decrease as K -fields are stretched farther laterally because the horizontal extent of the low- K units increases, which increases the tortuosity of vertical flowpaths and may force more water to flow through low- K units, rather than around them. Kh remains nearly constant as K -fields are stretched, resulting in increasing anisotropy with the areal extent of the K -field. Anisotropy greater than 10,000:1 is found in the 60 km×60 km fields in two cases and in the 80 km×80 km field in one case. The variability in anisotropy between the three fields is a result of differences in the lithologic proportions as well as the lateral and vertical spatial structure, which are quantified, in part, as variograms (see also e.g., Desbarats 1987).

The horizontal variogram range for each field is an indication of the lateral extent of the layers. The horizontal clay indicator variogram range for the 250×250 m simulation grid is 115, 85, and 135 m for fields 1, 2, and 3, respectively. Stretching the ranges onto the linearly interpolated grid size corresponding to 10,000:1 anisotropy (grid sizes of 42, 68, and 59 km, respectively) results in clay range values of 20, 23, and 32 km, for the three fields, respectively. It is reasonable to believe that confining units extend 20–30 km in the Bengal Basin, based on the understanding of Basin development presented in the section [Geology](#).

The necessity of upscaling in large-scale numerical simulations is illustrated by the relative size of the K -fields and the Bengal Basin model. Each field had 1.5 million cells, making even this simple flow simulation computationally

expensive. If the same level of detail were maintained, the full model of the Bengal Basin (2.8×10^5 km² in area) would require 44 of the 80 km×80 km K -fields, or 66 million cells, and more if the entire vertical extent were to be represented.

Comparison to analytical statistical model: streamline method

An alternative conceptualization of the stratified aquifer system can aid in understanding and support the results of the analysis. An analytical solution for the equivalent vertical hydraulic conductivity of a petroleum reservoir containing thin, discontinuous, flow barriers (shales) oriented horizontally and distributed randomly within a matrix was developed by Begg and King (1985). The solution assumes that the barriers are impermeable and rectangular in shape, and that flow can be approximated as streamlines through the matrix, around the shale barriers; thus K_v is controlled by the flowpath tortuosity in the geologic structure. Begg et al. (1985) showed that the solution, though derived for impermeable shales, is valid for a K contrast between barrier and matrix of greater than 100. For the case of an isotropic matrix, the equation is:

$$K_{v_e} = \frac{K(1 - F_s)}{(1 + f\bar{d})^2}, \quad (6)$$

where K_{v_e} is the equivalent vertical hydraulic conductivity, K is the isotropic matrix (sand) hydraulic conductivity, F_s is the fraction of shale, f is the number of shales per unit depth, and is \bar{d} the horizontal extent of the streamtube. For a three-dimensional system and isotropic shale shape, \bar{d} is equal to one third the average length of a shale unit.

The K values assigned to clay, silt, and sandy clay (low- K facies) are more than 100 times less than the K values assigned to sand and gravel (high- K facies), with the exception of silt and fine sand, between which the K contrast is 65. Silt comprises merely 1% of the aquifer system, based on the driller log data, and low- K units can be approximated as long and thin; thus the streamline method can be applied to obtain an alternative estimate of vertical anisotropy. The number of low- K facies units per unit depth can be obtained from the driller log data, with an average of 0.03 units/m, or 3 low- K units per 100 m of aquifer sediment. The low- K fraction is 38%. The parameter not available from the data, again, is the horizontal extent of the low- K units. An edge length of 12.6 km, or \bar{d} of 4.2 km, results in a K_{v_e} value of 5.2×10^{-8} , and an anisotropy of 10,000. Low- K unit edge lengths of 40 km and 10 km result in anisotropy values of 99,700 and 6,300, respectively.

In comparison with the values obtained from the analysis of flow through the three K -fields, these values of anisotropy are high, indicating that the low- K units in the groundwater simulation of these K -fields do conduct

some of the groundwater flow. This can also be seen by looking at the ratio of anisotropy values as the geostatistical K-fields are stretched. According to Eq. 6, the value of Kv_e (and therefore anisotropy) should increase by a factor of 4 if the low- K unit edge length is doubled. The ratio of anisotropy values obtained for the K-fields (Table 5) indicates that doubling the edge length of the K-fields only increases anisotropy by a factor of 3.3 or less, and this value decreases as the K-fields become larger. Thus, a greater proportion of vertical flow goes through low- K units as their horizontal extent increases.

Discussion and conclusions

On a regional scale, the unconsolidated sediments of the Bengal Basin may be considered a single aquifer. Fine-grained units are numerous, but there is currently a lack of evidence of laterally extensive confining units. Instead, sedimentation controlled by active tectonics, dynamic fluvial deposition, and fluctuating sea level has likely resulted in a stratified, heterogeneous aquifer fabric in which fine-grained units are laterally discontinuous. Such heterogeneity is not mappable on a regional scale for direct representation in a regional numerical groundwater model. Instead, discontinuous layers of fine and coarse sediments are represented with an equivalent hydraulic conductivity that is considerably lower in the vertical than the horizontal direction. With this conceptual model as a foundation, three approaches to estimation of equivalent hydrogeologic parameters were carried out using three independent types of data: (1) inverse modeling using shallow, transient hydraulic head measurements produced estimates of horizontal and vertical hydraulic conductivity as well as specific yield, one equivalent value for each parameter over the Basin; (2) groundwater age estimates from ^{14}C measurements were used to manually calibrate a steady-state model to produce estimates of Basin-wide equivalent horizontal and vertical hydraulic conductivity; (3) an analysis of lithology using driller logs produced estimates of horizontal and vertical hydraulic conductivity at every driller log location, allowing statistical analysis among eight physiographic regions of the Basin and estimates of the average parameter values in each.

Despite the diverse sets of sparse data and approaches to estimation, the three methods produced similar parameter value estimates and indicate that the ratio of horizontal to vertical hydraulic conductivity is near to or greater than 10^4 . The consistency of this value with the conceptual model and the driller log data was corroborated by comparison with an analytical expression and by simulation of groundwater flow through geostatistically generated fields that fit the lithologic data and the conceptual model described previously.

The strong large-scale vertical anisotropy of the Bengal Basin aquifer system is expected to be an important control on the distribution of groundwater flow in this

fluvio-deltaic aquifer that is subject to very low topographic and hydraulic gradients as driving forces. This analysis shows that some layers of low hydraulic conductivity (e.g., clay) must extend laterally for about 20–30 km in order to generate anisotropy of the magnitude found by parameter estimation. This may explain the conceptual model of hydrogeologists in the region, that there are several aquifers at depth, separated by confining units. A low-conductivity layer of the preceding extent would cause, in a high-conductivity layer below, a short-term appearance of confined-aquifer-like behavior in response to short-term localized stresses above it. Determination of the response of the larger system would be difficult from short-term local measurements, as are usually obtained. However, because the confining units are only of limited lateral extent, with greater time and more widely distributed stresses, aquifer responses would tend toward that of a single anisotropic aquifer of much greater spatial scale, as postulated in this study.

The results of this analysis can guide data collection for better parameter estimation in the future. Transient hydraulic head data, collected on a regular basis (e.g., daily) at greater depths than done to date would allow better estimation of regional aquifer parameters that control flow below the current horizon of shallow pumping in the aquifer. Additional ^{14}C , geochemical and isotopic data collected at depth (> 100 m) in more locations would provide important information on the functioning of the flow systems in the aquifer. Finally, careful studies of the aquifer fabric in several physiographic regions, involving installation of boreholes, logging sediment lithology, determination of hydraulic conductivity of individual lithologies, and geophysical logging would allow the correlation structure of the aquifer system and the equivalent parameter values to be more accurately determined. Where a local confining unit is thought to be laterally extensive, this should be confirmed by carefully correlating among its appearances in boreholes via other corroborative information, including paleontological, mineralogical, geochemical, and isotopic data. Geophysical surveys using widely applied technology such as ground-penetrating radar or seismic profiling would also provide useful information on the extent and connectivity of confining units. Although difficult and costly to apply over large areas, strategic collection of additional data could result in more confident parameter estimates as well as identification of regional differences, trends, and variability throughout the Basin.

More generally, this work illustrates the value of particular data types in parameter estimation and the effectiveness of different estimation strategies when faced with limited data. The utility of inverse modeling methods is dependent on the quality of both the model and the data, as well as on the sensitivity of measurements to the target parameters. In this case, deep hydraulic head and groundwater age data exhibit the highest sensitivity for estimating large-scale groundwater flow to deep parts of aquifer systems; they provide information on large regions

of the groundwater flow system. In contrast, driller-log data provide specific information at single locations in space, allowing point-wise estimation of properties and understanding of spatial variability or continuity. In this case, the sparse nature of the data prevented estimation of lateral spatial continuity across the Basin, but vertical spatial correlation and regional differences were well-resolved. Improved understanding of the advantages and limitations of estimation methods and utility of the data used in them can guide data collection in future studies such that it is optimal for the estimation methods used, the particular parameters to be estimated, and their spatial location and extent.

Acknowledgements Thanks are due to K.M. Ahmed (University of Dhaka), A. Zahid (Bangladesh Water Development Board and University of Dhaka), M.A. Hoque (Bangladesh University of Engineering and Technology), S.P. Sinha Ray (Centre for Groundwater Studies), P. Sikdar and P. Sahu (Indian Institute of Social Welfare and Business Management) and S. Chakraborty (Bengal Engineering and Science University) for technical advice and ongoing cooperation; to J. Whitney and D. Clark (US Geological Survey) for initiating and supporting this project; to G. Howard, R. Johnston, and R. Nickson for their support; to M. Allison (Tulane University) and S. Goodbred (Vanderbilt University) for insights into Bengal Basin geology; to R. Ababou (Institut de Mecanique des Fluides de Toulouse) and A. Boucher (Stanford University) for discussions on geostatistics; to L.N. Plummer (US Geological Survey) for providing ^{14}C corrections; and to C. West, A.H.M. Shamsuddin, and J. Coleman of UNOCAL for geologic information. The project was funded by UNICEF, the Arsenic Policy Support Unit of the British Department for International Development, the US Agency for International Development, and the US Geological Survey. Thanks are also due to the Government of Bangladesh through the Department of Public Health and Engineering and the Bangladesh Water Development Board. We also thank the technical reviewers of this manuscript. This work was conducted in part while H.M. was a National Research Council Postdoctoral Research Associate at the US Geological Survey (2005–2006).

References

- Ababou R (1996) Random porous media flow on large 3-D grids: numerics, performance, and application to homogenization. In: Wheeler MF (ed) *Environmental studies: mathematical, computational, and statistical analysis*. Springer, New York, pp 1–25
- Aggarwal PK, Basu AR, Poreda RJ, Kulkarni KM, Froehlich K, Tarafdar SA, Ali M, Ahmed N, Hussain A, Rahman M, Ahmed SR (2000) Isotope hydrology of groundwater in Bangladesh: implications for characterization and mitigation of arsenic in groundwater. IAEA-TC Project BGD/8/016, IAEA, Vienna
- Ahmed KM, Bhattacharya P, Hasan MA, Akhter SH, Alam SMM, Bhuyian MAH, Imam MB, Khan AA, Sracek O (2004) Arsenic enrichment in groundwater of the alluvial aquifers in Bangladesh: an overview. *Appl Geochem* 19:181–200
- Alam MK, Hasan AKMS, Khan MR, Whitney JW (1990) Geological map of Bangladesh. Geological Survey of Bangladesh, Dhaka
- Alam M, Alam MM, Curray JR, Chowdhury MLR, Gani MR (2003) An overview of the sedimentary geology of the Bengal Basin in relation to the regional tectonic framework and basin-fill history. *Sediment Geol* 155:179–208
- Allison MA (1998) Geologic framework and environmental status of the Ganges-Brahmaputra Delta. *J Coast Res* 14(3):826–836
- Allison MA, Khan SR, Goodbred SL Jr, Kuehl SA (2003) Stratigraphic evolution of the late Holocene Ganges-Brahmaputra lower delta plain. *Sediment Geol* 155:317–342
- Begg SH, King PR (1985) Modelling the effects of shales on reservoir performance: calculation of effective vertical permeability, paper SPE 13529 presented at the SPE Reservoir Simulation Symposium, Dallas, TX, 10–13 February 1985
- Begg SH, Cheng DM, Haldorsen HH (1985) A simple statistical method for calculating the effective vertical permeability of a reservoir containing discontinuous shales, paper SPE 14271 presented at the 1985 SPE Annual Technical Conference and Exhibition, Las Vegas, NV, 22–25 September 1985
- Bethke CM, Johnson TM (2002) Paradox of groundwater age. *Geology* 30:107–110
- BGS, DPHE (2001) Arsenic contamination of groundwater in Bangladesh. In: Kinniburgh DG, Smedley PL (eds) *British Geologic Survey Report WC/00/19*, vols. 1–4, British Geologic Survey, Keyworth, UK
- BWDB (2002) Upazila-wise tubewell data. Bangladesh Water Development Board, Ground Water Hydrology Division-II, Dhaka
- Carrera J, Alcolea A, Medina A, Hidalgo J, Slooten LJ (2005) Inverse problem in hydrogeology. *Hydrogeol J* 13:206–222
- Coleman JM (1969) Brahmaputra River: channel processes and sedimentation. *Sediment Geol* 3(2–3):129–239
- de Marsily Gh, Delay F, Goncalves J, Renard Ph, Teles V, Violette S (2005) Dealing with spatial heterogeneity. *Hydrogeol J* 13:161–183
- Desbarats AJ (1987) Numerical estimation of effective permeability in sand-shale formations. *Water Resour Res* 23(2):273–286
- Deshmukh DS, Prasad KN, Niyogi BN, Biswas AB, Guha SK, Seth NN, Sinha BPC, Rao GN, Goswami AB, Rao PN, Narasimhan TN, Jha BN, Mitra SR, Chatterjee D (1973) Geology and groundwater resources of the alluvial areas of West Bengal. *Bulletins of the Geological Survey of India, Series B No. 34*, Geological Survey of India, New Delhi
- Devore JL (2000) *Probability and statistics for engineering and the sciences*. Duxbury, Pacific Grove, CA
- Domenico PA, Schwartz FW (1998) *Physical and chemical hydrogeology*, 2nd edn. Wiley, New York
- DPHE (1999) Overview, production tube wells, eighteen district towns project phase III. Department of Public Health Engineering, Dhaka, Bangladesh
- DPHE (2006) Final Report on Development of Deep Aquifer Database and Preliminary Deep Aquifer Map (First Phase), Department of Public Health and Engineering, Government of the People's Republic of Bangladesh, Arsenic Policy Support Unit, and JICA, Dhaka, Bangladesh
- EROS (2002) Shuttle Radar Topography Mission (SRTM) Elevation Data Set. National Aeronautics and Space Administration (NASA), German Aerospace Center (DLR), Italian Space Agency (ASI), From: the National Center for Earth Resources Observations and Science, US Geological Survey, Sioux Falls, SD
- Fontes J-C, Garnier J-M (1979) Determination of the initial ^{14}C activity of the total dissolved carbon: a review of the existing models and a new approach. *Water Resour Res* 15(2):399–413
- Goodbred SL Jr, Kuehl SA (2000) The significance of large sediment supply, active tectonism, and eustasy on margin sequence development: late quaternary stratigraphy and evolution of the Ganges-Brahmaputra Delta. *Sediment Geol* 133:227–248
- Goodbred SL Jr, Kuehl SA, Steckler MS, Sarker MH (2003) Controls on facies distribution and stratigraphic preservation in the Ganges-Brahmaputra Delta sequence. *Sediment Geol* 155:301–316
- Goovaerts P (1997) *Geostatistics for natural resources evaluation*. Oxford University Press, New York, 483 pp
- Harbaugh AW, Banta ER, Hill MC, McDonald MG (2000) MODFLOW-2000, the US Geological Survey modular groundwater model: user guide to modularization concepts and the groundwater flow process: US Geological Survey Open-File Rep 00–92

- Hill MC, Banta ER, Harbaugh AW, Anderman ER (2000) MODFLOW-2000, the US Geological Survey modular ground-water model: user guide to the observation, sensitivity, and parameter-estimation processes and three post-processing programs. US Geol Surv Open-File Rep 00-184
- Hunt RJ, Feinstein DT, Pint CD, Anderson MP (2006) The importance of diverse data types to calibrate a watershed model of the Trout Lake Basin, northern Wisconsin, USA. *J Hydrol* 321:286–296
- Hussain MM, Abdullah SKM (2001) Geological setting of the areas of arsenic safe aquifers. Report of the ground water task force. Interim Report No. 1, Ministry of Local Government, Rural Development & Cooperatives, Local Government Division, Bangladesh
- JICA (2002) The study on the ground water development of deep aquifers for safe drinking water supply to arsenic affected areas in western Bangladesh. Final report, Kokusai Kogyo, Mitsui, Tokyo
- Johnson SY, Alam AMN (1990) Sedimentation and tectonics of Sylhet Trough, northeastern Bangladesh. US Geol Surv Open-File Rep 90-313
- Journal AG, Alabert FG (1990) New method for reservoir mapping. *J Pet Technol* 42(2):212–218
- Keating EH, Robinson BA, Vesselinov VV (2005) Development and application of numerical models to estimate fluxes through the regional aquifer beneath the Pajarito Plateau. *Vadose Zone J* 4:653–671
- Khan FH (1991) *Geology of Bangladesh*. Wiley, New Delhi, India
- Kuehl SA, Allison MA, Goodbred SL, Kudrass H (2005) The Ganges-Brahmaputra Delta: concepts, models, and examples. *SEPM Spec Publ* 83:413–434
- Michael HM, Voss CI (2008) Evaluation of the sustainability of deep groundwater as an arsenic-safe resource in the Bengal Basin. *PNAS* 105(25):8531–8536
- Michael HM, Voss CI (2009) Controls on groundwater flow in the Bengal Basin of India and Bangladesh: regional modeling analysis. *Hydrogeol J*. doi:10.1007/s10040-008-0429-4
- Morgan JP, McIntire WG (1959) Quaternary geology of the Bengal Basin, East Pakistan and India. *Bull Geol Soc Am* 70:319–342
- MPO (1985) *Geology of Bangladesh*, Technical Report No. 4, Ministry of Irrigation, Water Development and Flood Control, Dhaka, Bangladesh
- MPO (1987) *The groundwater resource and its availability for development*, Technical Report No. 5, Ministry of Irrigation, Water Development and Flood Control, Dhaka, Bangladesh
- Naff RL, Haley DF, Sudicky EA (1998) High-resolution Monte Carlo simulation of flow and conservative transport in heterogeneous porous media, 1: methodology and flow results. *Water Resour Res* 34(4):663–677
- Persitz FM, Wandrey CJ, Milici RC, Manwar A (2001) *Digital Geologic and Geophysical Data of Bangladesh*. US Geol Surv Open File Rep 97-470H
- Pint CD, Hunt RJ, Anderson MP (2003) Flowpath delineation and ground water age, Allequash Basin, Wisconsin. *Ground Water* 41(7):895–902
- Poeter EP, Hill MC (1997) Inverse models: a necessary next step in ground-water modeling. *Ground Water* 35(2):250–260
- Pollock DW (1994) User's guide for MODPATH/MODPATH-LOT, version 3: a particle tracking post-processing package for MODFLOW, the US Geological Survey finite-difference ground-water flow model. US Geol Surv Open-File Rep 94-464
- Rahman AA, Ravenscroft P (2003) Groundwater resources and development in Bangladesh, background to the arsenic crisis, agricultural potential and the environment. University Press, Dhaka, Bangladesh
- Ravenscroft P, Burgess WG, Ahmed KM, Burren M, Perrin J (2005) Arsenic in groundwater of the Bengal Basin, Bangladesh: distribution, field relations, and hydrogeological setting. *Hydrogeol J* 14:727–751
- Remy N (2004) The Stanford geostatistical earth modeling software (sgems): a tool for new algorithms development. In: Leuangthong O, Deutsch CV (eds) *Geostatistics Banff 2004*. Kluwer, Dordrecht, The Netherlands, pp 865–872
- Renard P, de Marsily G (1997) Calculating equivalent permeability: a review. *Adv Water Resour* 20(5–6):253–278
- Sanchez-Vila X, Guadagnini A, Carrera J (2006) Representative hydraulic conductivities in saturated groundwater flow. *Rev Geophys* 44, RG3002
- Sanford W (1997) Correcting for diffusion in Carbon-14 dating of ground water. *Ground Water* 35:537–361
- Sanford WE, Plummer LN, McAda DP, Bexfield LM, Anderholm SK (2004) Hydrochemical tracers in the middle Rio Grande Basin, USA: 2, calibration of a groundwater-flow model. *Hydrogeol J* 12:389–407
- Sanz E, Voss CI (2006) Inverse modeling for seawater intrusion in coastal aquifers: insights about parameter sensitivities, variances, correlations and estimation procedures derived from the Henry problem. *Adv Water Resour* 29(3):439–457. doi:10.1016/j.advwatres.2005.05.014, 439-457
- Sarris TS, Paleologos EK (2004) Numerical investigation of the anisotropic hydraulic conductivity behavior in heterogeneous porous media. *Stoch Environ Res Risk Assess* 18:188–197
- Shamsuddin AHM, Brown TA, Rickard M (2002) Resource studies indicate large gas potential in Bangladesh. *Oil Gas J* 100(16):48–52
- Sikder AM, Alam MM (2003) 2-D modelling of the anticlinal structures and structural development of the eastern fold belt of the Bengal Basin, Bangladesh. *Sediment Geol* 155:209–226
- Uddin A, Lundberg N (1999) A paleo-Brahmaputra? Subsurface lithofacies analysis of Miocene deltaic sediments in the Himalayan-Bengal system, Bangladesh. *Sediment Geol* 123:239–254
- Uddin A, Lundberg N (2004) Miocene sedimentation and subsidence during continent-continent collision, Bengal Basin, Bangladesh. *Sediment Geol* 164:131–146
- Umitsu M (1993) Late Quaternary sedimentary environments and landforms in the Ganges Delta. *Sediment Geol* 83:177–186
- van Geen A, Zheng Y, Versteeg R, Stute M, Horneman A, Dhar R, Steckler M, Gelman A, Small C, Ahsan H, Graziano J, Hussein I, Ahmed KM (2003) Spatial variability of arsenic in 6000 tube wells in a 25 km² area of Bangladesh. *Water Resour Res* 39(5), 1140. doi:10.1029/2002WR001617
- Wen X-H, Gomez-Hernandez J (1996) Upscaling hydraulic conductivities in heterogeneous media: an overview. *J Hydrol* 183(1):ix–xxxii
- Williamson AK, Grubb HF, Weiss JS (1990) Ground-water flow in the Gulf Coast aquifer systems, south central United States: a preliminary analysis. US Geol Surv Water Resour Invest Rep 89-4071
- Zhang Y, Gable CW, Person M (2006) Equivalent hydraulic conductivity of an experimental stratigraphy: implications for Basin-scale flow simulations. *Water Resour Res* 42, W05404. doi:10.1029/2005WR004720
- Zinn BA, Konikow LF (2007) Potential effects of regional pumpage on groundwater age distribution. *Water Resour Res* 43, W06418. doi:10.1029/2006WR004865